



The following Communications have been judged by at least two referees to be “very important papers” and will be published online at www.angewandte.org soon:

T. Amaya, H. Sakane, T. Hirao*

A Concave-Bound CpFe Complex of Sumanene as a Dished-Up Metal in a π -Bowl

A. M. Brizard, M. C. Stuart, K. J. van Bommel, A. Friggeri, M. R. de Jong, J. H. van Esch*

Nanostructures by Orthogonal Self-Assembly of Hydrogelators and Surfactants

H.-C. Chiu,* Y.-W. Lin, Y.-F. Huang, C.-K. Chuang, C.-S. Chern
Polymer Vesicles Containing Small Vesicles within Interior Aqueous Compartments and pH-Responsive Transmembrane Channels

M. J. Hangauer, C. R. Bertozzi*

A FRET-Based Fluorogenic Phosphine for Live-Cell Imaging with the Staudinger Ligation

A. Baumgartner, K. Sattler, J. Thun, J. Breu*

A Novel Route to Microporous Materials: Oxidative Pillaring of Micas

M. Kirchmann, K. Eichele, F. M. Schappacher, R. Pöttgen, L. Wesemann*

Octahedral Coordination Compounds of the Ni, Pd, Pt Triad

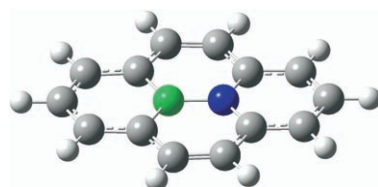
Books

Plenty of Room for Biology at the Bottom Ehud Gazit

reviewed by B. Samorí _____ 236

One of these bonds is not like the others:

Cyclic π systems in which B–N units replace their isoelectronic C–C counterparts have intrigued chemists and materials scientists for decades. The recent report of Piers et al. on the synthesis, crystal structure, and optical properties of 10a-aza-10b-borapyrenes (see picture) represents a major breakthrough in this field.



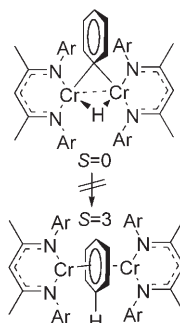
Highlights

Heteropolycyclic Aromatics

Z. Liu, T. B. Marder* _____ 242–244

B–N versus C–C: How Similar Are They?

Spin blocking: Facile reductive C–H elimination is a key step in chromium-catalyzed selective trimerization of olefins. The direct conversion (see scheme) is prevented by the change in spin states. This Highlight also describes the latest advances in the mechanistic understanding of the catalytic trimerization with a focus on spin states.



Reductive C–H Eliminations

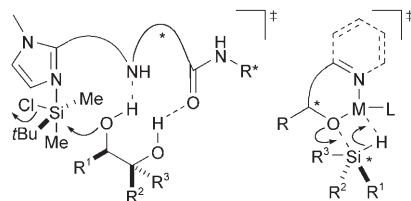
R. D. Köhn* _____ 245–247

Reactivity of Chromium Complexes under Spin Control

Asymmetric Catalysis

S. Rendler, M. Oestreich* — 248–250

Kinetic Resolution and Desymmetrization by Stereoselective Silylation of Alcohols



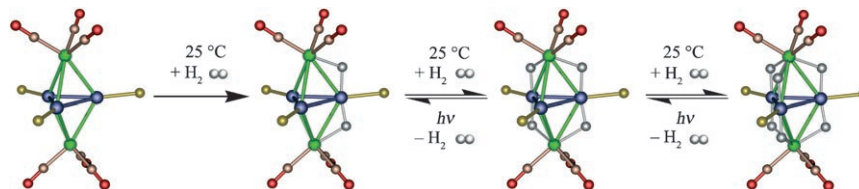
Watch out asymmetric acylation! Non-enzymatic kinetic resolution and desymmetrization by the asymmetric acylation of alcohols has found its rival in the related silylation of alcohols. The scheme shows the two-point binding of the substrate in catalyst- (left) and reagent-controlled stereoselective silylation (right).

Minireviews

Hydrogen Storage

R. D. Adams,* B. Captain — 252–257

Hydrogen Activation by Unsaturated Mixed-Metal Cluster Complexes: New Directions



Recent studies of unsaturated mixed-metal cluster complexes containing platinum and bulky phosphine ligands for hydrogen activation are reviewed (see picture; Pt blue, Rh green, P yellow, O red,

C light brown, H gray). A summary of some related studies on bimetallic cooperativity and trimetallic nanoparticles for catalytic hydrogenation is also included.

Reviews

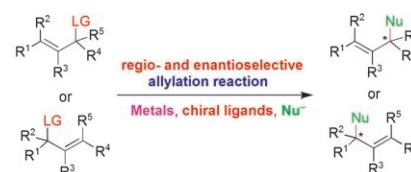
Synthetic Methods

Z. Lu, S. Ma* — 258–297



Metal-Catalyzed Enantioselective Allylation in Asymmetric Synthesis

Chiral carbon centers can be constructed in a highly stereoselective manner by the reaction of allylic substrates containing a leaving group with a range of nucleophiles in the presence of metal complexes and chiral ligands.



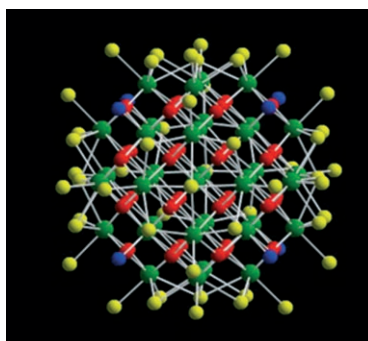
Communications



Actinide Chemistry

L. Soderholm,* P. M. Almond,
S. Skanthakumar, R. E. Wilson,
P. C. Burns* — 298–302

The Structure of the Plutonium Oxide Nanocluster $[\text{Pu}_{38}\text{O}_{56}\text{Cl}_{54}(\text{H}_2\text{O})_8]^{14-}$



Oxide inside: The structure of a plutonium(IV) oxide nanocluster (see picture; Pu green, O red and blue, Cl yellow) has been determined by single-crystal diffraction in the solid state and verified in aqueous solution by high-energy X-ray scattering. The nanoparticles are composed of 38 Pu ions arranged in an oxide lattice with a structure slightly distorted from the fluorite phase seen in PuO_2 . An absorption spectrum of the Pu clusters in solution is consistent with the classic Pu-polymer optical response.

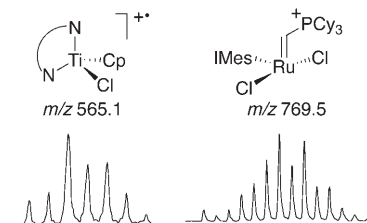
For the USA and Canada:

ANGEWANDTE CHEMIE International Edition (ISSN 1433-7851) is published weekly by Wiley-VCH, PO Box 191161, 69451 Weinheim, Germany. Air freight and mailing in the USA by Publications Expediting Inc., 200

Meacham Ave., Elmont, NY 11003. Periodicals postage paid at Jamaica, NY 11431. US POSTMASTER: send address changes to *Angewandte Chemie*, Wiley-VCH, 111 River Street, Hoboken, NJ 07030. Annual subscription price for institutions: US\$ 7225/6568 (valid for print and

electronic / print or electronic delivery); for individuals who are personal members of a national chemical society prices are available on request. Postage and handling charges included. All prices are subject to local VAT/sales tax.

Getting the air out: A bottleneck in transition-metal chemistry is the laborious process of identifying organometallic molecules. Anaerobic, charge-transfer MALDI-MS is a powerful new tool for observation of these reactive, often fragile species. Examples are drawn from catalysts relevant to olefin metathesis, hydrogenation, polymerization, and cyclopropanation. IMes = *N,N'*-bis-(mesityl)imidazol-2-ylidene.



Inert-Atmosphere MALDI-MS

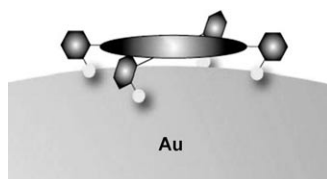


M. D. Eelman, J. M. Blacquiere,
M. M. Moriarty, D. E. Fogg* — 303–306

Shining New Light on an Old Problem:
Retooling MALDI Mass Spectrometry for
Organotransition-Metal Catalysis



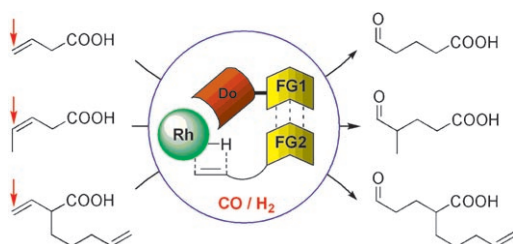
Bound through S–Au bonds, multidentate macrocyclic porphyrin thioester derivatives densely protect Au nanoparticles in a face-coordination fashion (see picture) to form quite stable Au⁰ porphyrins. The spectroscopic Soret-band intensity can be tuned by the distance between the porphyrin ring and the Au surface.



Gold(0) Porphyrins

M. Kanehara, H. Takahashi,
T. Teranishi* — 307–310

Gold(0) Porphyrins on Gold
Nanoparticles



Supramolecular Catalysis

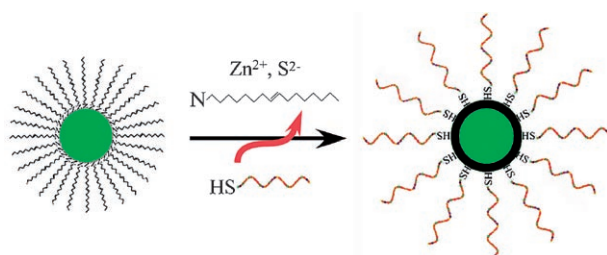
T. Šmejkal, B. Breit* — 311–315

A Supramolecular Catalyst for
Regioselective Hydroformylation of
Unsaturated Carboxylic Acids



The quest to capture the catalytic power of enzymes is one of the great challenges of modern chemistry. A novel system inspired by the principles of enzymatic catalysis combines recognition of the

substrate and transition-metal catalysis (see scheme; Do = donor, FG = functional group) and mimics enzyme properties—high efficiency, substrate selectivity, and reaction-site selectivity.



Quantum Dots

Q. Wang,* Y. Liu, Y. Ke, H. Yan* — 316–319

Quantum Dot Bioconjugation during
Core–Shell Synthesis

One small step: A facile and robust one-step method for creating stable, water-soluble quantum dot (QD)–biomolecule conjugates is described. DNA molecules

can be readily attached to QDs during core–shell synthesis (see picture of DNA functionalization of a CdSe@ZnS core–shell QD).

Incredibly reader-friendly!



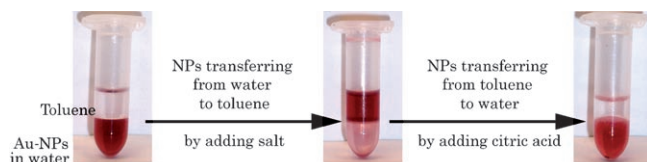
An aesthetically attractive cover picture that arouses curiosity, a well-presented and most informative graphical table of contents, and carefully selected articles that are professionally edited give *Angewandte Chemie* its distinctive character, which allows both easy browsing and further in-depth reading. Nearly 20 well-trained chemists, as well as eight further associates, work week in and week out to assemble reader-friendly issues and daily Early View articles online.



GESELLSCHAFT
DEUTSCHER CHEMIKER



service@wiley-vch.de
www.angewandte.org



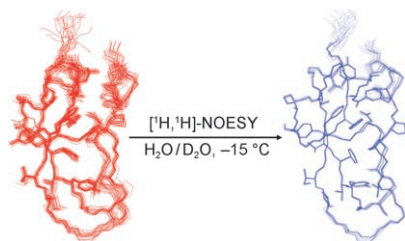
To cap it all: With the aid of stimuli-responsive polymer capping, gold nanoparticles (Au-NPs) can be highly colloidal stable in both aqueous and organic

media. They spontaneously and reversibly cross water/oil interfaces in both directions upon formation of a biphasic salty water–oil system (see picture).

Nanoparticle Transport

E. W. Edwards, M. Chanana, D. Wang,*
H. Möhwald 320–323

Stimuli-Responsive Reversible Transport of Nanoparticles Across Water/Oil Interfaces

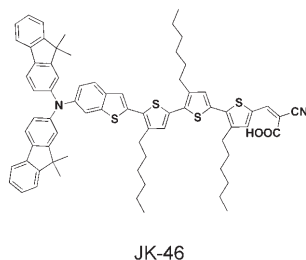


Fidelity without frostbite: Refinement of an NMR solution structure of 6-kDa protein BPTI determined at 36 °C (see picture, red) with NOE distance constraints measured in supercooled water at –15 °C increased precision of backbone and core side-chain coordinates about twofold (blue). In contrast to cryogenic X-ray crystallography (–150 °C), supercooling to about –15 °C hardly affects the conformation of flexibly disordered surface side chains.

Protein Structures

Y. Shen, T. Szyperski* 324–326

Structure of the Protein BPTI Derived with NOESY in Supercooled Water: Validation and Refinement of Solution Structures



A sense for sensitizers: Devices based on JK-46 (see structure) and a volatile electrolyte yielded an extremely high overall conversion efficiency of 8.6% under AM 1.5 sunlight. Solar cells fabricated employing the JK-46 sensitizer and a solvent-free ionic-liquid electrolyte gave an efficiency of over 7% and demonstrated excellent stability under light soaking at 60 °C for 1000 h.

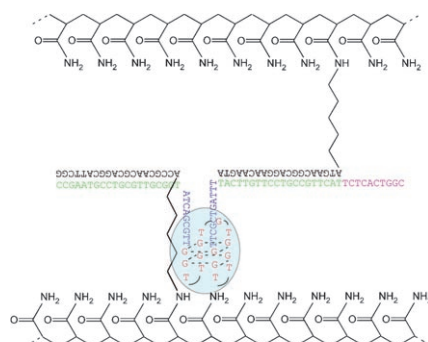
Solar Cells

H. Choi, C. Baik, S. O. Kang, J. Ko,*
M.-S. Kang, Md. K. Nazeeruddin,*
M. Grätzel 327–330

Highly Efficient and Thermally Stable Organic Sensitizers for Solvent-Free Dye-Sensitized Solar Cells



Cross-links holding on, then letting go: Polyacrylamide main chains were branched with DNA strands, which could be gelatinized by DNA base pairing with a thrombin-bound cross-linking strand (see scheme). A complementary DNA strand can form a duplex with the cross-linking strand to dissolve the hydrogel and release the thrombin.



DNA Hydrogels

B. Wei, I. Cheng, K. Q. Luo,
Y. Mi* 331–333

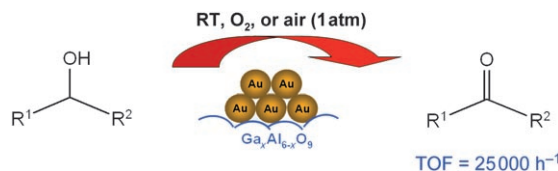
Capture and Release of Protein by a Reversible DNA-Induced Sol–Gel Transition System

Aerobic Oxidation

F. Z. Su, Y. M. Liu, L. C. Wang, Y. Cao,*
H. Y. He, K. N. Fan ————— 334–337



Ga–Al Mixed-Oxide-Supported Gold Nanoparticles with Enhanced Activity for Aerobic Alcohol Oxidation



Toward greener organic synthesis: A high activity for the aerobic oxidation of alcohols is achieved under base-free and ambient conditions by using gold catalysts supported on mesostructured

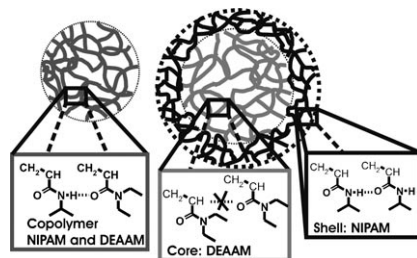
γ -Ga₂O₃/Al₂O₃ solid solutions (see picture). The enhanced activity is attributed to the extraordinary alcohol-dehydrogenation activity of gallia-based mixed oxides.

Microgels

M. Keerl, V. Smirnovas, R. Winter,
W. Richtering* ————— 338–341



Interplay between Hydrogen Bonding and Macromolecular Architecture Leading to Unusual Phase Behavior in Thermosensitive Microgels

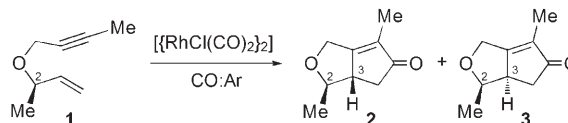


In a depressed state: The intra- and intermolecular hydrogen-bonding pattern of microgels comprising *N*-isopropylacrylamide (NIPAM) and *N,N*-diethylacrylamide (DEAAM) can be determined by FTIR spectroscopy. In contrast to core-shell systems (see picture, right), an increase in intramolecular hydrogen bonding in copolymer microgels (left) favors polymer–polymer interactions and leads to a marked depression of the phase-transition temperature.

Diastereoselective Carbocyclization

H. Wang, J. R. Sawyer, P. A. Evans,*
M.-H. Baik* ————— 342–345

Mechanistic Insight into the Diastereoselective Rhodium-Catalyzed Pauson–Khand Reaction: Role of Coordination Number in Stereocontrol



$$2:3 \begin{cases} 22:1 & \text{CO:Ar} = 100:0 \\ 6:1 & \text{CO:Ar} = 5:95 \end{cases}$$

How much CO? Theoretical analysis of the origin of diastereocontrol in the rhodium-catalyzed Pauson–Khand reaction (see scheme) provides two mechanistic scenarios in which optimum selectivity can be attributed to a five- rather

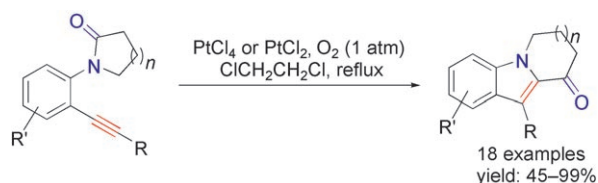
than a four-coordinate organorhodium complex. The relative population of these complexes is related to carbon monoxide concentration, a finding which is in contrast to phosphine-containing rhodium(I) complexes.

Transition-Metal Catalysis

G. Li, X. Huang, L. Zhang* — 346–349

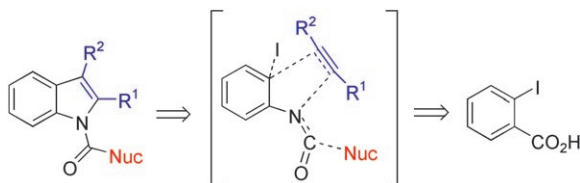


Platinum-Catalyzed Formation of Cyclic-Ketone-Fused Indoles from *N*-(2-Alkynylphenyl)lactams



An oxygen atmosphere aids the efficient formation of highly substituted ring-fused indoles by the versatile title reaction through an initial cyclization followed by the sequential migration of two groups. The cycloisomerization can be viewed as a

net intramolecular insertion of one end of the alkyne into the lactam amide bond with concurrent migration of the substituent at the alkyne terminus (see scheme; $n = 0–2$; R = alkyl, alkenyl, aryl, H; R' = OMe, Br, CO₂Et).



A synergism: The multicomponent assembly of an alkyne, a nucleophile, and a carboxylic acid gave indole derivatives in good yield and high regioselectivity by a one-pot Curtius rearrangement/palladium-catalyzed indolization process (see

scheme). A synergistic effect was observed; the by-product of the first reaction served as a reagent for the second step. The first synthesis of indole *N*-carboxamide derivatives by heteroannulation is also described.

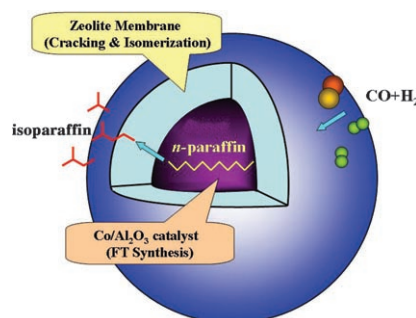
Multicomponent Reactions

O. Leogane, H. Lebel* 350–352

One-Pot Multicomponent Synthesis of Indoles from 2-Iodobenzoic Acid



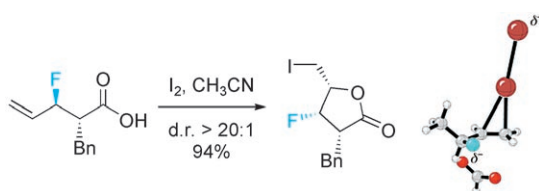
A well-wrapped catalyst: Coating an H-beta zeolite membrane onto the surface of a preshaped Co/Al₂O₃ pellet leads to a novel core/shell catalyst with a confined reaction environment which shows excellent selectivity for the synthesis of isoparaffins from syngas (see picture; FT = Fischer–Tropsch). Long-chain hydrocarbon formation is totally suppressed by the zeolite membrane. This kind of membrane catalyst could be extended to various other consecutive reactions by modifying the shell membrane and the core catalyst.



Core/Shell Catalysts

J. Bao, J. He, Y. Zhang, Y. Yoneyama, N. Tsubaki* 353–356

A Core/Shell Catalyst Produces a Spatially Confined Effect and Shape Selectivity in a Consecutive Reaction



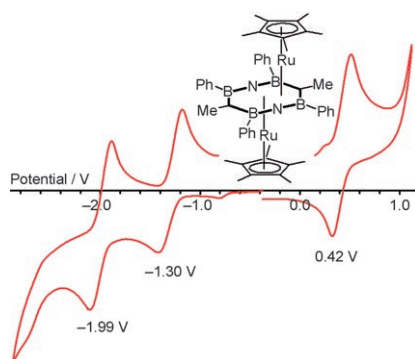
An inside job: β -Fluorinated lactones and tetrahydrofurans are synthesized by iodocyclization of various allylic fluorides. The fluorine substituent acts as a highly efficient *syn*-stereodirecting group for the

ring closure. The experimental results combined with theoretical studies provide evidence in support of an “*inside* fluoro effect” to account for the sense and level of stereocontrol of these reactions.

Stereoelectronic Effects

M. Tredwell, J. A. R. Luft, M. Schuler, K. Tenza, K. N. Houk, V. Gouverneur* 357–360

Fluorine-Directed Diastereoselective Iodocyclizations



Open, sesame: The reaction of a heterobicyclic pentalenediyl-like Me₂Ph₄B₄N₂C₂ dianion with [(C₅Me₅)RuCl]₄ cleaves the N–N bond of the ligand and affords a pseudo-triple-decker sandwich complex containing a B₄N₂C₂ middle deck (see picture). This eight-membered ring features nearly linear B–N–B moieties and brings the ruthenium centers unusually close. Cyclic voltammetry indicates efficient electron delocalization over the framework.

Sandwich Complexes

H. V. Ly, H. M. Tuononen, M. Parvez, R. Roesler* 361–364

Unusual B₄N₂C₂ Ligand in a Ruthenium Pseudo-Triple-Decker Sandwich Complex Displaying Three Reversible Electron-Transfer Steps

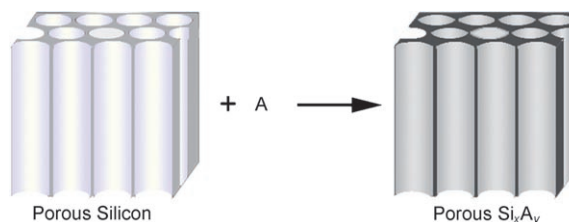


Membranes

Y. J. Yang, G. W. Meng,* X. Y. Liu,
L. D. Zhang ————— 365–367



Converting Free-Standing Porous Silicon
into Related Porous Membranes



Like a chip off the old block: Compound porous membranes Si_xA_y , such as Si_3N_4 , SiC , and Zn_2SiO_4 , have been synthesized by in situ conversion of porous silicon (PS) films (see picture). The resultant

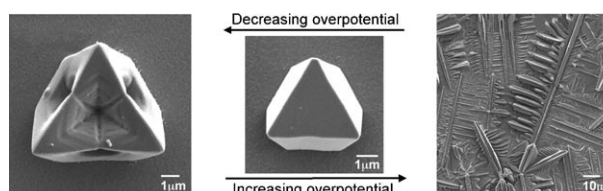
membranes inherit the morphology and microstructure of the mother PS films and have potential applications in filters, catalytic supports, and sensing materials.

Crystal Shape Control

M. J. Siegfried, K.-S. Choi* — 368–372



Elucidation of an Overpotential-Limited Branching Phenomenon Observed During the Electrocrystallization of Cuprous Oxide



Molecular bonsai: Depending on the reaction conditions, the growth of copper(I) oxide crystals proceeds by an overpotential-limited or a conventional diffu-

sion-limited dendritic branching mechanism (see picture). Faceting and branching are critically effected by the pH value and overpotential.

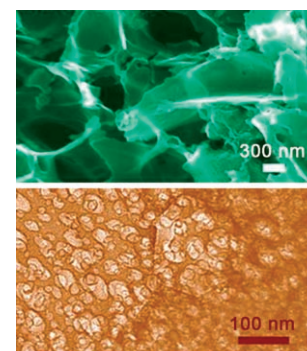
Energy Storage

D.-W. Wang, F. Li, M. Liu, G. Q. Lu,
H.-M. Cheng* ————— 373–376



3D Aperiodic Hierarchical Porous Graphitic Carbon Material for High-Rate Electrochemical Capacitive Energy Storage

Electrochemical capacitors: A hierarchical porous graphitic carbon material, composed of macroporous ion-buffering microreservoirs, ion-transporting channels, and localized graphitic wall structures, is presented (see images; top: 3D skeleton, bottom: carbon platelet). The properties of this new material combine to overcome the electrode kinetic problems normally found in electrochemical capacitors, thus resulting in an excellent high-rate energy-storage performance.

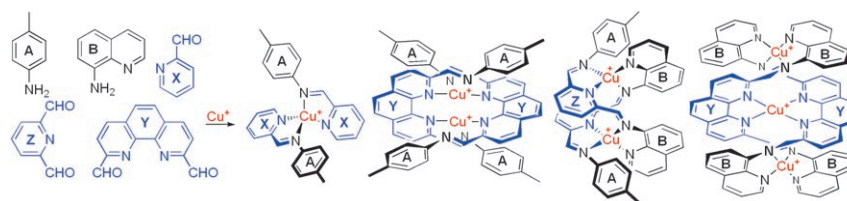


Systems Chemistry

R. J. Sarma, J. R. Nitschke* — 377–380

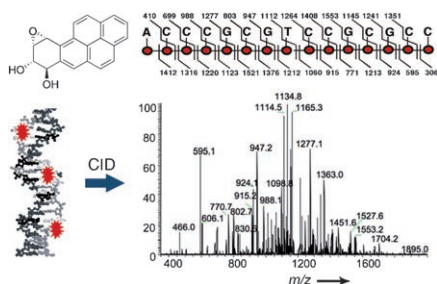


Self-Assembly in Systems of Subcomponents: Simple Rules, Subtle Consequences



All together now: Five subcomponents (see scheme) come together cleanly with Cu^{I} to form simultaneously all four product structures shown. Simply by changing the stoichiometry, any given subset

of product structures is accessible. To explain the observed selectivity, it is necessary to consider the stability not only of individual products, but of the system as a whole.

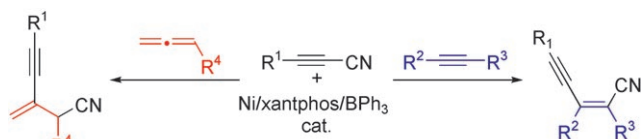


Map reading: Alkylation of a 15-base-pair double-stranded oligonucleotide modified with the carcinogen (±)-anti-benzo[a]pyrene diol epoxide (see picture) or N-hydroxy-4-aminobiphenyl is mapped by liquid chromatography–tandem mass spectrometry and collision-induced dissociation (CID). The method does not require prior DNA cleavage or hydrolysis.

DNA Damage

G. Chowdhury,
F. P. Guengerich* 381–384

Direct Detection and Mapping of Sites of Base Modification in DNA Fragments by Tandem Mass Spectrometry



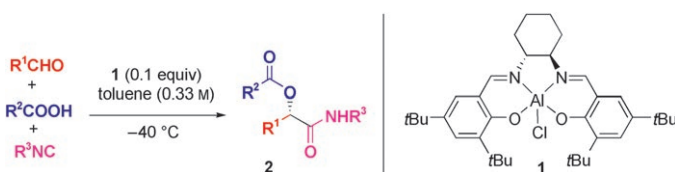
Adding across: A C(sp)–C(sp) bond of alkynyl cyanides is activated by nickel/Lewis acid catalysis derived from [Ni(cod)₂] and BPh₃, and the alkynylcyanation reaction of alkynes and 1,2-dienes

is achieved by the binary catalysis for the first time to give a range of functionalized conjugated enyne molecules with defined stereo- and regioselectivities.

Enyne Synthesis

Y. Nakao,* Y. Hirata, M. Tanaka,
T. Hiyama* 385–387

Nickel/BPh₃-Catalyzed Alkynylcyanation of Alkynes and 1,2-Dienes: An Efficient Route to Highly Functionalized Conjugated Enynes



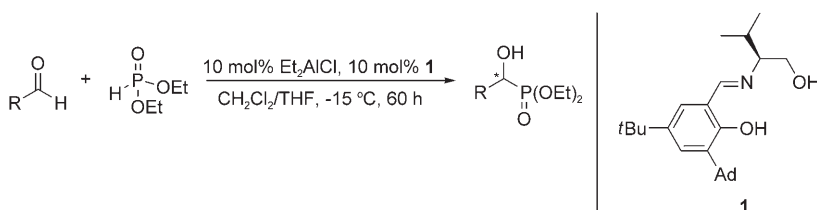
Make it enantioselective: The [(salen)-Al^{III}Cl] complex **1** catalyzes the title reaction of an aldehyde, a carboxylic acid, and an isocyanide to afford α-acyloxamides **2** with good to excellent enantioselectivity. A

variety of nonchelating substrates can be used to generate the versatile chiral products. R¹ = alkyl; R² = alkyl, alkenyl, aryl; R³ = alkyl, aryl.

Asymmetric Catalysis

S.-X. Wang, M.-X. Wang,* D.-X. Wang,
J. Zhu* 388–391

Catalytic Enantioselective Passerini Three-Component Reaction



Active in dimeric form: A tridentate Schiff base aluminum(III) complex has been applied in the asymmetric hydrophosphonylation of various aldehydes, giving the corresponding products in good yields with good to excellent *ee* values (up to

97%). The strong positive nonlinear effect, along with high-resolution MS analyses, indicates that the reaction is performed in the presence of a dimeric aluminum species. Ad = adamantyl.

Asymmetric Catalysis

X. Zhou, X. H. Liu, X. Yang, D. J. Shang,
J. G. Xin, X. M. Feng* 392–394

Highly Enantioselective Hydrophosphonylation of Aldehydes Catalyzed by Tridentate Schiff Base Aluminum(III) Complexes



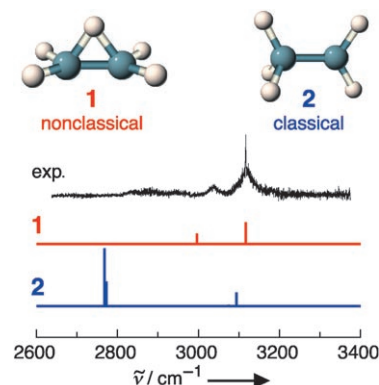
Carbocations

H.-S. Andrei, N. Solcà,
O. Dopfer* 395–397



IR Spectrum of the Ethyl Cation: Evidence for the Nonclassical Structure

Argon tagging allowed the IR spectrum of the ethyl cation $C_2H_5^+$ to be inferred by resonant IR photodissociation spectroscopy of weakly bound $C_2H_5^+ \cdot Ar$ complexes (see picture). The experimental spectrum closely resembles the theoretical spectra of **1** and **1**·Ar but shows large deviations from the spectrum predicted for **2**, and thus it provides the first direct spectroscopic evidence for the nonclassical structure **1** of protonated ethene.

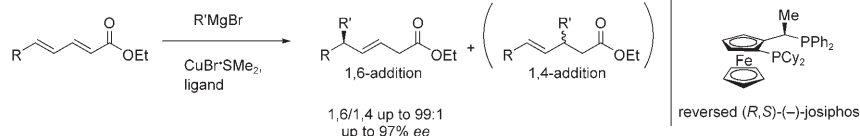


Asymmetric Catalysis

T. den Hartog, S. R. Harutyunyan, D. Font,
A. J. Minnaard,* B. L. Feringa* 398–401



Catalytic Enantioselective 1,6-Conjugate Addition of Grignard Reagents to Linear Dienoates



Dual function of catalyst: Both regio- and enantioselectivity are dictated by Cu catalysis using the reversed josiphos ligand. This allows enantioselective 1,6-addition

of Grignard reagents to acyclic $\alpha,\beta,\gamma,\delta$ -unsaturated esters monosubstituted at the β and δ positions (see scheme).

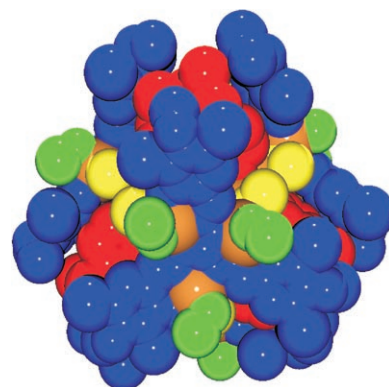
Cage Compounds

I. M. Oppel (née Müller),*
K. Föcker 402–405



Rational Design of a Double-Walled Tetrahedron Containing Two Different C_3 -Symmetric Ligands

Two is better than one: The predictability of supramolecular coordination compounds relies on an exact match between the ligands used and the steric demand of the metal center. However, the use of two different C_3 -symmetric ligands results in a double-walled tetrahedron (see picture; inside: red, outside: blue; orange Zn^{2+} , yellow methanolate, green MeOH or H_2O) that does not contain a perfectly matched ligand–metal pair.

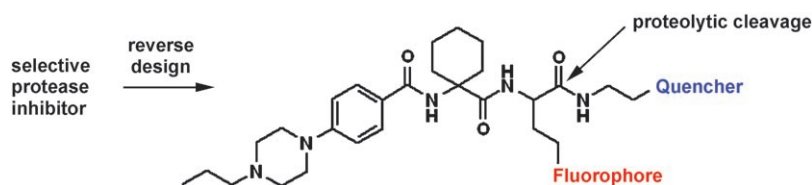


Fluorescence Probes

A. Watzke, G. Kosec, M. Kindermann,
V. Jeske, H.-P. Nestler, V. Turk, B. Turk,*
K. U. Wendt* 406–409

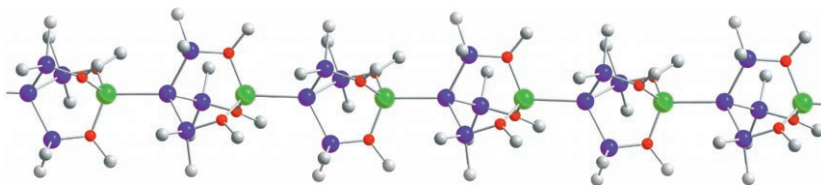


Selective Activity-Based Probes for Cysteine Cathepsins



By “reverse design”: The core structures of protease inhibitors, whose selectivity has been optimized by extensive medicinal chemistry, have been redesigned into selective protease substrates by replacing the reactive electrophilic group (e.g.

nitrile) with a cleavable peptide bond. Attachment of appropriate reporter groups yields cell-permeable activity-based probes for the cellular imaging of selected cysteine cathepsins.



Chain gang: Introducing methoxy groups into $(\text{Me}_3\text{Si})_4\text{Si}$ and treatment with alkali metal alkoxides leads to hitherto unknown zwitterionic alkali metal silanides $[(\text{MeO-Me}_2\text{Si})_3\text{SiM}]$ with a bicyclocubane (Li, Na) or heterocubane (K) structure. The lithium

and sodium compounds form infinite chains in the solid state (see picture: green Li, blue Si, red O, gray C) and dissociate in THF solutions into zwitterionic monomers.

Silanide Clusters

C. Krempner,* M. H. Chisholm,
J. Gallucci _____ 410–413

The Multidentate Ligand
 $(\text{MeOMe}_2\text{Si})_3\text{Si}^-$: Unusual Coordination
Modes in Alkali Metal Silanides



Supporting information is available on the WWW
(see article for access details).



A video clip is available as Supporting Information
on the WWW (see article for access details).

Sources

Product and Company Directory

You can start the entry for your company in “Sources” in any issue of
Angewandte Chemie.

If you would like more information, please do not hesitate to contact us.

Wiley-VCH Verlag – Advertising Department

Tel.: 0 62 01 - 60 65 65

Fax: 0 62 01 - 60 65 50

E-Mail: MSchulz@wiley-vch.de

Service

Spotlights Angewandte's
Sister Journals _____ 234–235

Keywords _____ 414

Authors _____ 415

Preview _____ 417



For more information on
Chemistry—An Asian Journal see
www.chemasianj.org